Escape through a time-dependent hole in the doubling map

Article *in* Physical Review E · December 2013

DOI: 10.1103/PhysRevE.89.052913 · Source: arXiv

4 authors, including:

André L P Livorati
São Paulo State University

Orestis Georgiou
Ultrahaptics Ltd

Edson D. Leonel
São Paulo State University

Escape through a time-dependent hole in the doubling map

André L. P. Livorati[1,2], Orestis Georgiou [2], Carl P. Dettmann[2] and Edson D. Leonel[3]
[1] *Instituto de Física - IFUSP - Universidade de São Paulo - USP Rua do Matão, Tr.R 187 - Cidade Universitária – 05314-970 – São Paulo – SP – Brazil – livorati@usp.br*
[2] *School of Mathematics - University of Bristol - Bristol BS8 1TW - United Kingdom*
[3] *Departamento de Física – UNESP – Universidade Estadual Paulista – Av. 24A, 1515 - Bela Vista - 13506-900 - Rio Claro - SP - Brazil*

We investigate the escape dynamics of the doubling map with a time-periodic hole. We use Ulam's method to calculate the escape rate as a function of the control parameters. We consider two cases, oscillating or breathing holes, where the sides of the hole are moving in or out of phase respectively. We find out that the escape rate is well described by the overlap of the hole with its images, for holes centred at periodic orbits.

PACS numbers: 05.45.Pq, 05.45.Tp

I. INTRODUCTION

One of the main recent problems of interest among physicists and mathematicians, is the study of dynamical systems with holes [1]. The introduction of these holes allows phase space orbits to escape, i. e., leak out according to some pre-existing escape condition, that could be related to some variable of the system dynamics. The leaking can happen in closed domain systems [2, 3] as well in unbounded domain systems [4, 5]. We search for the statistical properties related to this leaking (escape), such as $\rho(n)$, which is the probability that an orbit remains inside the domain of the system until a time n, i. e. until the escape occur. A natural question is raised then, that is what would be the decay rate of $\rho(n)$? The most important aspects on such leaking analysis are that the escape rate is very sensitive to what kind of dynamics the system under study presents. If we have a strong chaotic behaviour, the decay is typically exponential [6], on the other hand, systems that present mixing properties, as stability islands, invariant curves and chaotic sea, the decay can be a mix of exponential with a power law [7]. Also, the escape rate can depend a lot of the position and size of the hole. Some applications of leaking systems, can be found in several areas of physics, as plasmas [8, 9], acoustic [10], optics [11, 12], fluids [13], among others.

In this paper we propose a different version of escape, where the hole is time dependent, in position and/or size, as the dynamics of the system evolves. We expect that this time-periodic leaking configuration would bring different aspects and properties to the survival probability, as well as influence the transport along the dynamics. We decided to start the investigations on this time-dependent hole in one of the most simple problems, the doubling map [14–17], which for a fixed hole case, the escape and transport properties are well known in the literature [18–20], so we can make a comparison with our results on the time-dependent hole. Also, once the periodic orbits may play an important role in the dynamics considering a system with a hole, as shown for the logistic map [21], and for the doubling mapping itself [5, 18–20], we aim to seek and understand their role in the escape for the time-dependent hole, and try to find some analytical expressions for the escape rates, as done previously [22, 23]. One can find a recent application in Quantum Mechanics for a time-dependent leaking system in Ref.[24].

This paper is organized as follows: In Sec.II we describe how the time-dependent hole is introduced, and some properties concerning the escape rate and the periodic orbits. The numerical and analytical results are shown in Sec.III. Finally some final remarks and conclusions are drawn in Sec.IV.

II. THE MAPPING, PROPERTIES AND THE TIME-DEPENDENT HOLE

The dynamical system under study here is the doubling map with a modulo one, also known as the Bernoulli shift, represented by the recurrence relation below

$$x_{n+1} = 2x_n \quad mod(1) \ . \tag{1}$$

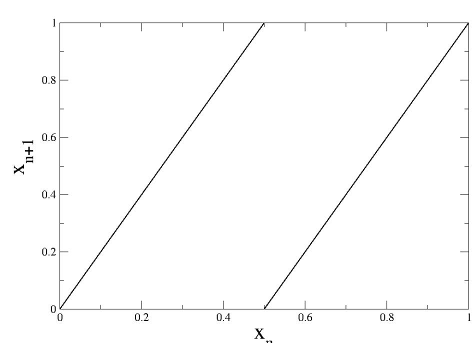

FIG. 1: *Phase space for the doubling map.*

The phase space is shown in Fig.1. Because of the simple nature of the dynamics when we consider the binary notation [5], it is easy to categorize the dynamics based on the initial condition. If the initial condition is irrational, which are almost all points in the unit interval, the dynamics is classified as non-periodic, which follows directly from the definition of an irrational number as one with a non-repeating binary expansion. This is classified as a chaotic case. However, if x_0 is rational, the image of x_0 contains a finite number of distinct values within the interval $[0, 1)$ and the forward orbit of x_0 is eventually periodic, with period equal to the period of the binary expansion of x_0. Particularly, if the initial condition is a rational number with a finite binary expansion of k bits, then after k iterations the iterates reach the fixed point 0; if the initial condition is a rational number with a k-bit transient ($k \geq 0$) followed by a p-bit sequence ($p > 1$) that repeats itself infinitely, then after k iterations the iterates reach a cycle of length m. Thus cycles of all lengths are possible [5]. Also, another way of representing the periodic orbits is

$$x_0 = \frac{q}{(2^p - 1)} \ , \tag{2}$$

where $q \in \mathbb{Z}$ and p is the period of the periodic orbit. So, for example, if we choose an initial condition with $q = 8$ and $p = 4$, it would be a period-4 orbit with dynamics evolving to $8/15 \to 1/15 \to 2/15 \to 4/15 \to 8/15$.

Once the main properties of the mapping are known, let us now introduce the escape in the dynamics, by considering a time-dependent hole, i. e., a hole whose position and/or size are varying periodically. We set a mean fixed position for the hole to oscillate, $\bar{x}$, that could be in the neighbourhood of a periodic orbit, or even the periodic orbit itself. Choosing the mean position around a periodic orbit allows us to compare the results we obtain with the results already known in the literature for the fixed hole position [18–20, 23].

So, once the mean position is set up, we may define the hole size. Since, this value should vary with time, we can work with an average size of the hole, which we will name as $\bar{h}$. So, two fixed positions for the hole to oscillates were set, and we define them as hole at the right h_r and hole at the left h_l, as they are set as

$$\begin{cases} h_r = \bar{x} + \bar{h}/2 \\ h_l = \bar{x} - \bar{h}/2 \end{cases} \tag{3}$$

Now we introduce the time dependence on the hole. Noting that we are dealing with a discrete recurrence relation (n), and not a continuous as time (t), we set that the hole dependence in relation to n. So, with a periodic oscillation, Eqs.(3) can be written as

$$\begin{cases} h_r(n) = h_r + \epsilon \cos(\omega n + \phi_r) \\ h_l(n) = h_l + \epsilon \cos(\omega n + \phi_l) \end{cases} \ , \tag{4}$$

where ϵ is the amplitude of oscillation of the holes, $\omega = (2\pi/\tau)$ is the frequency of oscillation and ϕ_l and ϕ_r are the initial phases of oscillation.

The value of the phases ϕ_l and ϕ_r, in particular, whether they are equal, will directly influence the value of the amplitude of oscillation ϵ. Figure 2 shows how the hole would oscillates according n evolves for a mean position around a period-4 orbit (8/15) and $\tau = 20$ for two different situations. If ϕ_l and ϕ_r are in phase as shown in Fig.2(a), the position of the hole is moving as n evolves, but it remains with the same size; here we have no limit for the value of ϵ, provided that is inside the domain of the doubling map. However, if ϕ_l and ϕ_r are not in phase, as shown in Fig.2(b), the hole size is moving, in a breathing way. Here we have the limit breathing case that is $\epsilon \leq \bar{h}/2$. In this limit, we have a tangency between $h_l(n)$ and $h_r(n)$, when the period is complete, where the hole vanishes momentarily. If we go beyond this limit, there would be some prohibited regions for the escape, and we are not considering this case in this paper.

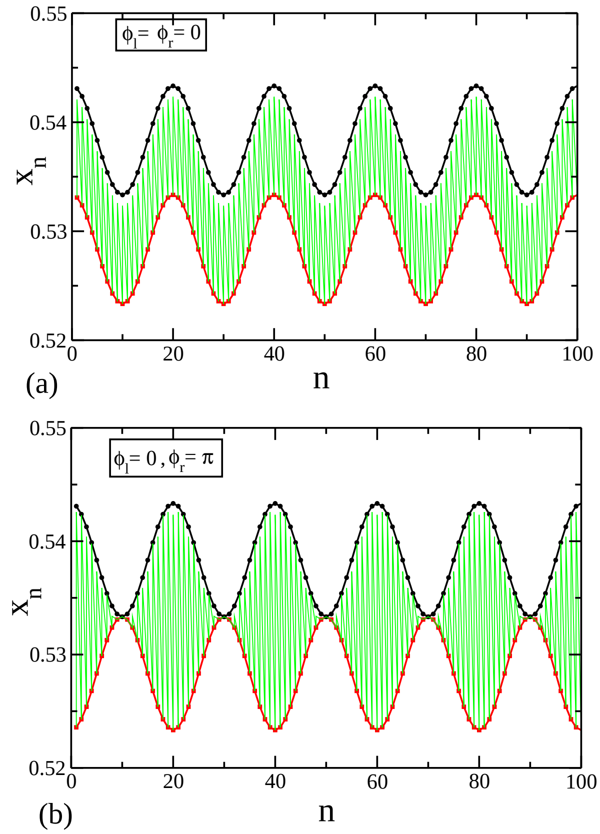

FIG. 2: *Evolution of the time-dependent hole for two combinations of the initial phases for a value of* $\tau = 20$ *and a mean value around a period-4 orbit located in* (8/15)*. In (a) both,* $h_l(n)$ *and* $h_r(n)$ *are in phase with each other, so the size of the hole is kept constant during the dynamics and only its position is moving. And in (b),* $h_l(n)$ *and* $h_r(n)$ *are not in phase, so the size of the hole is varying, but the average hole* $\bar{h}$ *is constant by period of oscillation. In this figure* $h_l(n)$ *is represented by the black line with bullets, and* $h_r(n)$*, setted as the red line with squares. The green dashed lines are the escape allowed region.*

III. METHODS, RESULTS AND DISCUSSIONS

In this section we will present analytical and numerical methods to evaluate the escape through the time-dependent hole. We investigate how the escape rate varies with the control parameters ϵ, τ and the combination of initial phases ϕ_l and ϕ_r. We also make frequent comparison with the static hole case.

A. Ulam's Method and Escape Rates

We made use of Ulam's Method to calculate the escape rates for the time-dependent hole. Ulam's method is a numerical scheme for approximating invariant densities of dynamical systems that can be made rigorous [25–29]. The phase space is partitioned into connected sets and an inter-set transition matrix is computed from the dynamics; an approximate invariant density is read off as the leading left eigenvector of this matrix. When a hole in phase space is introduced, one instead searches for conditional invariant densities and their associated escape rates [26–33]. In other words, we divide the space X into a fine partition X_i, and assume that the probability of a transition from i to j is given by the proportion of X_i that is mapped into X_j, that is

$$\rho_{ij} = \frac{|X_i \cap f^{-1}(X_j)|}{|X_i|} \ . \tag{5}$$

If we consider the static hole case, we would expect an exponential escape rate, that may depend on the hole position and its size, as studied before in [5, 18–20] for the same doubling map. The escape rate is

$$\gamma = -\lim_{n\to\infty} \frac{1}{n} \ln \rho(n) \ . \tag{6}$$

For a time-dependent hole, we find an exponential decay as in Eq.(6), but the time-dependence can also be more complicated, as discussed in Sec.III.C,

We are considering the two different cases of initial phases of ϕ_l and ϕ_r, as shown in Fig.2 in a separate way. Let us first address the case $\phi_l = \phi_r$ where only the hole position is moving and its size $\bar{h}$ is kept constant, Fig. 3 shows how these escape rates behave for some different average hole sizes, different values of amplitude of oscillation ϵ and different values of τ. For this figure, we decided to keep the mean value of the hole position $\bar{x} = 8/15$. In later sections, we address other mean values of the hole $\bar{x}$. As expected in Figs.3(a,c) with an average hole of $\bar{h} = 0.1$, we have a much faster decay, than in Figs.3(b,d), where the average hole is $\bar{h} = 0.01$. However, one can also notice that depending on the combination of ϵ and τ parameters, we may have a faster or slower escape, as shown in Figs.3(a,c), where for a bigger value of $\epsilon = 0.4$ which basically contains the whole domain of

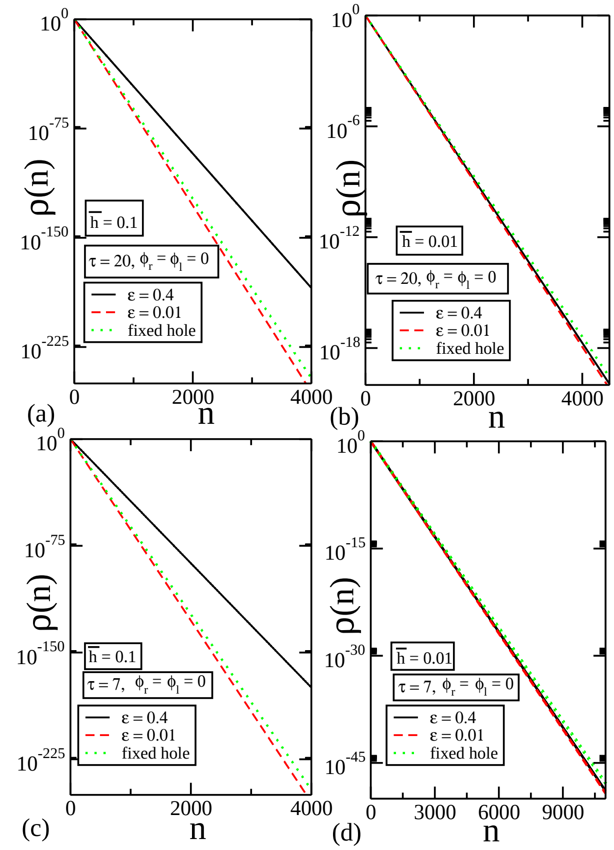

FIG. 3: *Survival probability curves for different values of the average moving hole with equal initial phases. In (a) and (b) we have $\tau = 20$, and in (c) and (d) $\tau = 7$. Also, we ranged the value of the amplitude of oscillation ϵ and made a comparison with the fixed hole case. Depending of the combination of ϵ and τ we may have faster or slower escape.*

the doubling map. In Table I one may find the value of the escape rate for some combinations of values of τ and ϵ.

h	τ	ϵ	γ
0.1	7.0	0.4	0.1004784(1)
0.1	7.0	0.01	0.1468975(5)
0.1	20.0	0.4	0.1061757(6)
0.1	20.0	0.01	0.1473164(5)
0.1	0.0	*fixed hole*	0.1418285(1)
0.01	7.0	0.4	0.01024197(3)
0.01	7.0	0.01	0.01030896(5)
0.01	20.0	0.4	0.01020202(1)
0.01	20.0	0.01	0.0103262(1)
0.01	0.0	*fixed hole*	0.0100119(1)

TABLE I: Value of the escape rate γ for a combination of ϵ and τ for two different hole sizes.

One can see, that the value of γ is proportional to the average hole size, that would be roughly expected according to Refs.[5, 17, 20, 23], but there are also significant

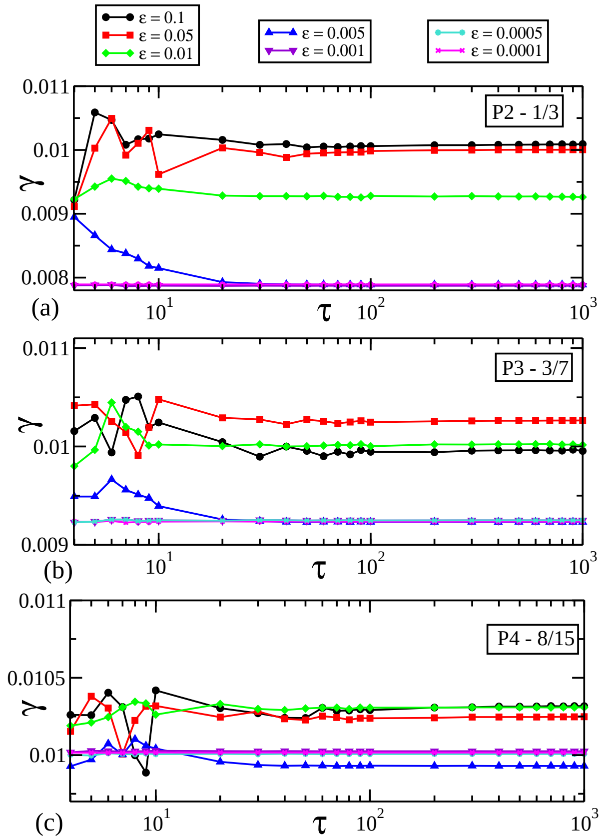

FIG. 4: *Variation of the escape rate γ as function of τ for several values of ϵ. Here the average hole is fixed at $\bar{h} = 0.01$, and we considered three different periodic orbits for the mean hole position. In (a) $\bar{x} = 1/3$, a period-2 orbit, in (b) $\bar{x} = 3/7$, a period-3 orbit, and finally in (c) $\bar{x} = 8/15$, a period-4 orbit. Notice that for high values of ϵ, for a small τ regime, the escape rate varies a lot, and as τ increases it bend towards an almost constant regime. For the limit $\epsilon \to 0$, the escape rate behaves as for a fixed hole for all values of τ.*

changes, depending of the combinations of the control parameters. In order to understand better how the escape rate varies with ϵ and τ, we plotted the value of the escape rate γ vs. τ for several values of ϵ, as shown in Fig.4. Here we keep the average hole size $\bar{h} = 0.01$ and consider at three different mean values for the hole to oscillate ($\bar{x}$) about three different periodic orbits. We see that for small values of τ, there is a large variation in the escape rate for all values of the mean hole, considering some high values of ϵ (say, above $\epsilon = 0.001$, which is 10 percent of the average hole size). These fluctuations can be explained, once ϵ is big enough and τ small, the hole is moving up and down really fast as the dynamics evolves, and during this movement, it can intercept several different periodic orbits, which may be one of the explanation for the variation of the escape rate. However, for high values of τ, the escape rate stays almost constant. This should be expected, since for high values of τ, the hole takes a time much larger then other timescales in this problem to change its position. Also, if we look for the curves with small values of ϵ, one can see that they stay in a constant regime for all values of τ, as once $\epsilon \to 0$, the moving hole starts to behave like a fixed hole. Comparing the limit of $\epsilon \to 0$ for Fig.4(a,b,c), we can see that the plateau where the escape rate stablish itself changes, when we consider a different periodic orbit. Indeed, as shown in [5, 19, 20, 23] the escape occurs faster through a hole wich contains large periodic orbits, and is slower if the hole contains a small periodic orbit. Recall that, according to the literature [5, 20, 23], the escape rate through a small hole covering a short periodic orbit is approximately given by

$$\gamma = \bar{h}(1 - \Lambda^{-1}) , \tag{7}$$

where $\Lambda = 2^p$, where p is the period of the periodic orbit. In Figure 4 we also observe higher order corrections to the expression presented in Eq.(7). These higher order corrections are specifically detailed in [20, 23].

B. Overlap Holes

We now develop an analytic approach where both ϕ_l and ϕ_r are in phase, as function of the control parameters τ and ϵ, using the overlap of the periodic orbits with the p application of the mapping in Eq.(1). The motivation for this kind of attempt came from Ref.[14], where an extensive analytical analysis is made concerning the escape rate on the doubling map. What the overlap hole approach do is basically a "correction" of Eq.(7), concerning the moving hole. Considering these overlaps, we can write the escape rate as

$$\gamma_{oh} = \bar{h}\left(1 - \frac{1}{\tau}\sum_{i=0}^{\tau-1}\frac{|T^p(H_i) \cap H_{i+p}|}{|T^p(H_i)|}\right) , \tag{8}$$

where the index oh means the overlap holes, H_i is the hole size in the i-th iteration, and H_{i+p} is the hole size considered on the $i+p$-th iteration.

We make a comparison of the results obtained considering the numerical simulations using the Ulam's Method, and analytical approach by the formula expressed in Eq.(8), for three different periodic orbits of low period and for two values of the average hole. The numerical data is represented by the full lines, as the analytical approach is given by the dotted lines. Although, both data follows a similar behaviour, as we increase the value of τ, one can see in Fig.5 that there is still a gap between the numerical data and the analytical approach. We can attribute these gaps, to higher order corrections, once for a fixed hole the escape rate should follow $\gamma = \bar{h}(1 - \Lambda) + o(\bar{h})$, where the corrections may lie on the form $\bar{h}^2 \ln \bar{h}$ [20]. The analytical data plotted in Fig.5 is hence adjusted according to

$$N[\gamma_{oh}(\tau)] = \gamma_{oh}(\tau) + \gamma_n(\infty) - \gamma_{oh}(\infty) , \tag{9}$$

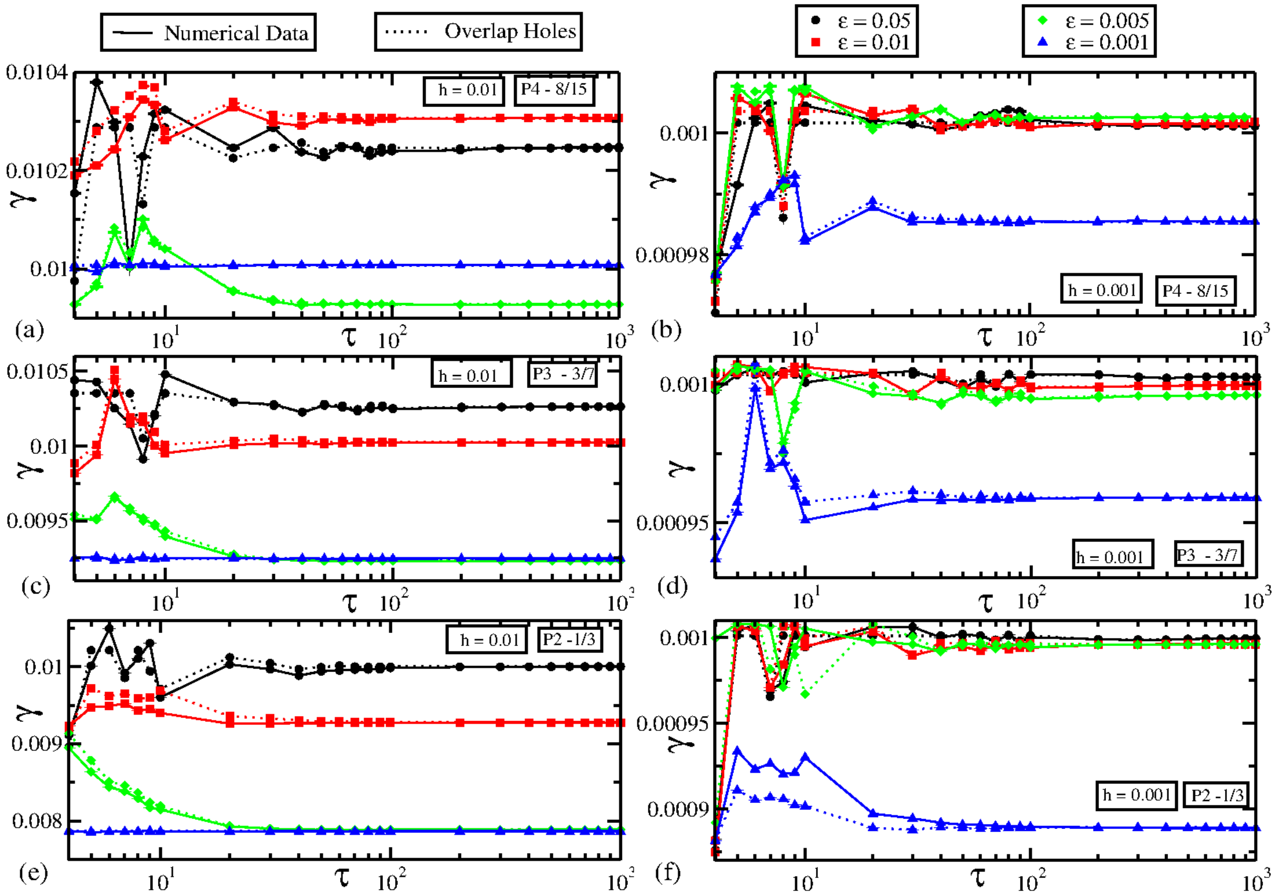

FIG. 5: *Comparison between the numerical data and the analytical approach for the overlap holes, given by Eqs.(8) and (9). In (a), (c) and (e) the average hole is $\bar{h} = 0.01$, and in (b), (d) and (f) we have $\bar{h} = 0.001$. Also, the numerical data is given by the full lines, and the analytical approach is given by the dotted lines. Bullets represent $\epsilon = 0.05$, squares $\epsilon = 0.01$, diamonds $\epsilon = 0.005$ and up triangles $\epsilon = 0.001$. The matching is really good for high values of τ, where the hole is moving slowly, but for low values of τ, where the hole is moving faster, there is still a gap between them.*

where, $N[\gamma_{oh}(\tau)]$ is the normalized escape rate considering the overlap holes approach, $\gamma_{oh}(\tau)$, is the analytical approach for the escape rate concerning the overlap holes according Eq.(8), γ_n, is the numerical escape rate obtained by the Ulam's method. The argument $\tau \rightarrow \infty$, is taken along an average between $\tau = 100$ and $\tau = 1000$, once the escape rate for this cases is almost constant. So, with this correction, the higher order effects are taken into account, and the matching between the numerical and the analytical approach concerning the overlap holes in Eqs.(8) and (9) occurs. However, one can still see small discrepancies for small values of τ, where the hole is moving too fast. These still need further investigation.

C. Breathing Hole

Now we address the case where $\phi_r = 0$, and $\phi_l = \pi$, shown in Fig.2(b), where the hole size is in constant change. Now, the hole is increasing and decreasing in a periodic way as n evolves, in a breathing way, but the average hole size is the same over the period of oscillation. Figure 6(a) shows the escape rate curve for this kind of moving hole, for some values of τ for a hole centred in a mean position of $\bar{x} = 8/14$. We can see that, in general it decays as an exponential envelope, but with a peculiarity: it decays in steps. The step obeys the period of oscillation of the moving hole, as shown in the comparison made in Figs.6(b,c). The steps can be basically explained by this comparison. Once the hole is increasing and decreasing, the rate of orbits that escape through it varies according to its size. So, when we have the tangency between both hole sides h_l and h_r, none of the orbits are escaping, so we have a constant plateau. On the other hand, when the hole is in its fully open size, we have a faster escape. Here we use the value of $\epsilon = \bar{h}/2$, that is the limit case, i. e., where h_r and h_l tangency each other, creating an instantaneous prohibited escape zone. If we had, a smaller value for ϵ, these step-like decays would be smoother, and in the limit that $\epsilon \to 0$, it would behave as a complete exponential curve decay.

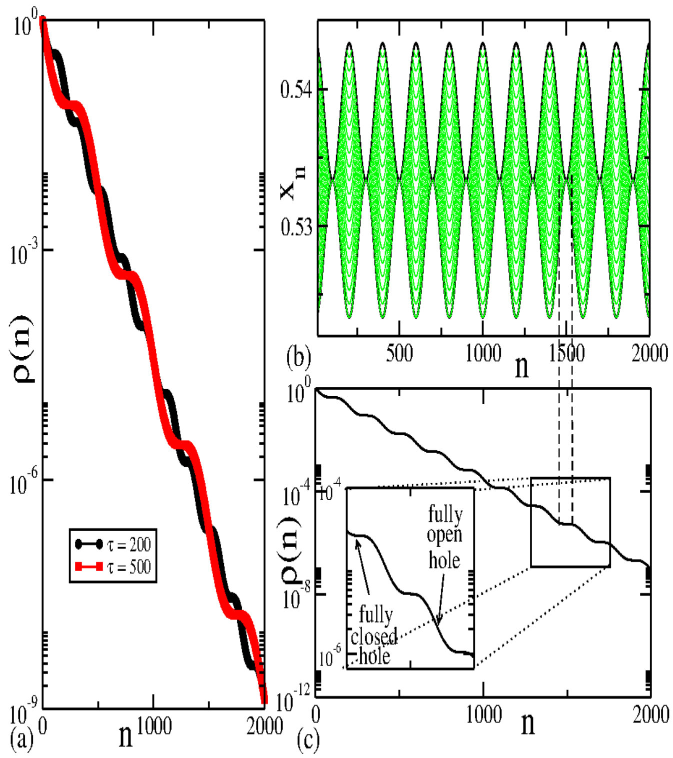

FIG. 6: *Step-like decay behaviour for the probability curves when $\phi_r = 0$ and $\phi_l = \pi$. We kept the average hole size constant in $\bar{h} = 0.01$ and $\epsilon = 0.005$, which is $\epsilon = \bar{h}/2$. In (a) we have $\tau = 200$ and $\tau = 500$. One can notice that the step-like decays of the survival probability follows the period of oscillation in a exponential envelope. In (b) and (c) we have a comparison of the hole behaviour with the probability decays. When the hole is fully open, we have a faster escape, and when the hole is fully closed (tangency), we have a constant plateau, where no orbits are escaping. The zoom window in (c) shows better this step-like behaviour.*

An attempt for an analytical approach for the breathing hole can be made. We have that the hole is $h(n) = h_r(n) - h_l(n)$, where $h_r(n)$ and $h_l(n)$ are given by Eq.(4), where the initial phases are $\phi_r = 0$ and $\phi_l = \pi$. So, we may say that the hole size obeys

$$h(n) = \bar{h} + 2\epsilon\cos(\omega n), \tag{10}$$

where $\omega = 2\pi/\tau$ and ϵ must not be bigger than $\bar{h}/2$.

Now, that the hole size is known we may propose the following expression where the decay of the survival probability as function of n, as shown in Fig.6, is given by

$$\frac{d\rho}{dn} = -\rho\left\{\left[\bar{h} + 2\epsilon\cos(\omega n)\right] \times P(noh)\right\} \ , \tag{11}$$

where $P(noh)$ is the probability of a point in the hole not overlapping with the hole on the $(n+p)$ iteration, just like we did for the the moving hole case, where again p is the period of the periodic orbit where the hole is centred. This probability is given by

$$P(noh) = \frac{\bar{h} + 2\epsilon\cos[\omega(n+p)]}{\bar{h} + 2\epsilon\cos(\omega n)} \times \frac{1}{\Lambda} \ . \tag{12}$$

Replacing the above expression and solving the separable equation, we have the following expression

$$\begin{aligned}\rho(n) = \exp\{&-\bar{h}n(1-\Lambda^{-1}) \\ &-\tfrac{2\bar{h}\epsilon}{\omega}[\sin(\omega n) + \tfrac{\sin[\omega(n+p)]}{\Lambda}]\} \ .\end{aligned} \tag{13}$$

In the above expression, the term $\bar{h}n(1-\Lambda^{-1})$ can be named as $\overline{\gamma(n)}$. Let us do an attempt to improve this expression making use of second order approximations. If we consider a fixed hole, the escape rate considering second order effects [14, 20] can be given by

$$\gamma_{fixed} = h\left(1-\Lambda^{-1}\right) + a_p h^2 \ln(h) \ , \tag{14}$$

where a_p is a constant that may depend on the p-periodic orbits. In order, to find the a_p value, we simulated for the several values of the fixed hole, and compared the numerical result of $\gamma = -\lim_{n\to\infty}\frac{1}{n}\ln\rho(n)$, with the analytical approach of Eq.(14), and found an average value for a_p, that is $a_2 \approx 1.812$, $a_3 \approx 2.055$ and $a_4 \approx 2.331$. We stress that the p-periodic orbits considered for the hole to be centred was the same ones used in the previous section.

Here the hole size is not constant and it is changing according n evolves, so we must assume that the escape rate is not constant either, as one can see in Fig.6. So, according to Eqs.(10) and (14), we may set

$$\gamma = h(n)\left(1-\Lambda^{-1}\right) + a_p h(n)^2 \ln[h(n)]. \tag{15}$$

Once we have an average value for the hole as $\bar{h}$, we can consider also an average over the escape rate as

$$\overline{\gamma} = \frac{\omega}{2\pi}\int_0^{\frac{2\pi}{\omega}} \gamma dn \ . \tag{16}$$

Replacing Eq.(10) and evaluating this average on Eq.(16), one can obtain

$$\begin{aligned}\overline{\gamma} = \bar{h}(1-\Lambda^{-1}) + a_p\{&\bar{h}[3\mu - \bar{h}(3\ln 4)] \\ -\epsilon^2(2\ln 16)\} - 2a_p&(2\epsilon^2+\bar{h}^2)\tfrac{\ln(\bar{h}+\mu)}{2} \ ,\end{aligned} \tag{17}$$

where $\mu = \sqrt{-4\epsilon^2 + \bar{h}^2}$. Now the step-like behaviour of $\rho(n)$ can be analytically expressed by the combinations of Eqs.(13) and (17), where higher order effects are considered

$$\rho(n) = \exp\{-\overline{\gamma}n - \tfrac{2\bar{h}\epsilon}{\omega}\{(\sin(\omega n) + \tfrac{\sin[\omega(n+p)]}{\Lambda})\} \ . \tag{18}$$

Figure 7 shows a comparison between the analytical (dotted lines) and the numerical data (full lines) for $\tau = 200$, for three distinct periodic orbits, concerning a hole size $\bar{h} = 0.01$. One can see that for the limit case $\epsilon = \bar{h}/2$ in Fig.7(a), the step-like decay in the exponential envelope is present according to the hole period of oscillation and the analytical approach matches reasonably well. If we decrease the amplitude of oscillation, to $\epsilon = 0.001$ as shows Fig.7(b), the survival probability curve presents a smooth behaviour concerning the step-like decays, and the exponential envelope is more dominant in the decay. For this case of smaller ϵ there is no more a instantaneous forbidden region in the hole evolution. However, concerning the zoom-in windows in Figs.7(c,d), there is still a little gap between the numerical and analytical data. We believe, that this gap may be due higher order effects, that may be introduced in Eq.(15) in order to improve the analytical expression.

IV. FINAL REMARKS AND CONCLUSIONS

We investigated the escape dynamics of the doubling map with a time-periodic hole with amplitude and period of oscillation, ϵ and τ respectively. We considered two distinct ways for the hole to oscillate: *(i)* keeping the same size and changing its position, and *(ii)* breathing case. This two kinds of hole are controlled by an initial phase ϕ_l and ϕ_r introduced in the time-dependent perturbation.

Using the Ulam's method to calculate the probability of escape, we found that it is basically exponential, and for case *(i)* it depends on the value of τ and ϵ. If we had a low τ, the hole is moving really fast and we observe some fluctuations on the escape rate γ vs. τ curves. If the hole is moving more slowly, the escape rate is correspondingly more slowly varying with τ. Also, for some high values of ϵ, the hole can intercept many periodic orbits, which can add even more fluctuations on the escape rate, and for $\epsilon \to 0$, it reduces to a fixed hole. In an attempt to explain these fluctuations, we introduced an analytical approach related to overlap holes. We observed that the numerical data and the analytical results, have excellent agreement if higher order effects are taken into account. Considering case *(ii)*, we observed that the probability decays according a step-like function in an exponential envelope, which follows the value of period of oscillation τ for the breathing hole. We set up an analytical approach for the step-like decay also considering the probability of overlap holes, and it reasonably matches with the numerical data. Also, in the limit $\epsilon \to 0$, the step-like is not observed and the survival probability decays as an exponential law.

We emphasize that the control parameters strongly affect the escape rate, for the moving hole, considering fast and slow moving hole, or the breathing case. As a next step, we would try to find the exactly higher order effects for the escape rate and improve the analytical expressions for both hole cases. Also, would be interesting to see how the escape rate would varies for periodic moving holes in more general systems than doubling map, and the effects if the hole perturbation is different from periodic, like a random one.

Acknowledgments

ALPL acknowledges CNPq and CAPES - Programa Ciências sem Fronteiras - CsF (0287-13-0) for financial support. EDL thanks FAPESP (2012/23688-5), CNPq and CAPES, Brazilian agencies. ALPL also thanks the University of Bristol for the kindly hospitality during his stay in UK. This research was supported by resources supplied by the Center for Scientific Computing (NCC/GridUNESP) of the São Paulo State University (UNESP). The authors are also grateful for fruitful discussions with Georgie Knight and Eduardo G. Altmann.

[1] E. G. Altmann, J. S. E. Portela and T. Tél, Rev. Mod. Phys., **85**, 869, (2013).
[2] Ying-Cheig Lai and Támas Tél, *Transient Chaos: Complex dynamics on finite-time scales*, Ap. Math. Sci., Vol. 173, 2011.
[3] P. Gaspard and G. Nicolis, Phys. Rev. Lett., **65**, 1693 (1990)
[4] P. Gaspard and D. Alonso Ramirez, Phys. Rev. A, **45**, 8383, (1992).
[5] L. A. Bunimovich and A. Yurchenko, Isr. J. Math, **182**, 229, (2011).
[6] E. D. Leonel and C. P. Dettmann, Phys. Lett. A, **376**, 1669, (2012).
[7] A. L. P. Livorati, T. Kroetz, C. P. Dettmann, I. L. Caldas and E. D. Leonel, Phys. Rev. E, **86**, 036203, (2012).
[8] J. S. E. Portela, I. L. Caldas and R. L. Viana, Int. J. Bifurcation and Chaos, **17**, 4067, (2011).
[9] D. del-Castillo-Negrete, B. A. Carreras, and V. E. Lynch, Phys. Rev. Lett., **94**, 065003 (2005).
[10] G. Tanner and N. Sondergaard, J. Phys. A, **40**, 443, (2007).
[11] E. G. Altmann, Phys. Rev. A, **79**, 013839, (2009).
[12] C. P. Dettmann, G. V. Morozov, M. Sieber and H. Waalkens, Phys. Rev. A, **80**, 063813, (2009).
[13] J. Scheneider, T. Tél and Z. Neufeld, Chaos, **17**, 3, 2007.
[14] G. Cristadoro, G. Knight and M. D. Esposti, J. Phys. A, **46**, 272001, (2013).
[15] P. Glendinning and N. Sidorov, Ergodic Theory and Dynamical Systems, available on CJO2013. doi:10.1017/etds.2013.98.
[16] R. A. Barrera, arXiv:1306.2054 [math.DS], (2013).
[17] L. A. Bunimovich, B. Webb, arXiv:1211.4617 [math.DS], (2013).
[18] G. Knight, O. Georgiou, C. P. Dettmann, R. Klages, Chaos, **22**, 023132, (2012).
[19] O. Georgiou, C. P. Dettmann, E. G. Altmann, Chaos, **22**, 043115, (2012).
[20] C. P. Dettmann, Nonlinearity, **26**, 307, (2013).

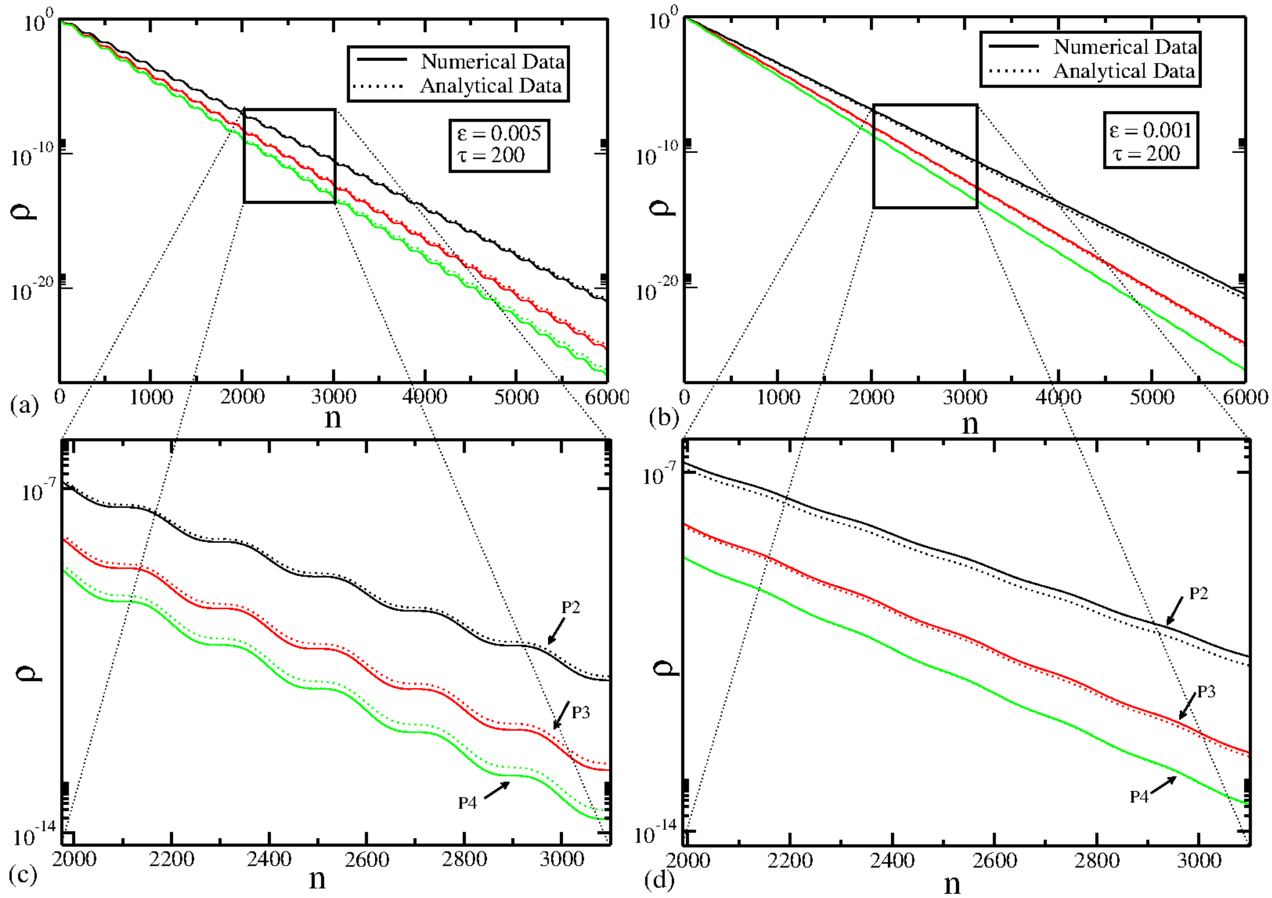

FIG. 7: *Comparison between the numerical step-like decays and the analytical approach given by Eq.(18) for* $\tau = 200$ *and* $\bar{h} = 0.01$. *In (a)* $\epsilon = 0.005$ *and in(b)* $\epsilon = 0.001$. *One can notice a remarkably good match between the numerical and the analytical data in the amplifications in (c) and (d).*

[21] V. Paar and N. Pavin, Phys. Rev. E, **55**, 4112, (1997).

[22] M. F Demers and L. S. Young, Nonlinearity, **19**, 377, (2006).

[23] G. Keller and C. Liverani, J. Stat. Phys., **135**, 519, (2009).

[24] A. Goussev, Phys. Rev. A, **87**, 053621, (2013).

[25] S. M. Ulam. *A collection of mathematical problems. Interscience Tracts in Pure and Applied Math- ematics*, no. 8. Interscience Publishers, New York-London, 1960.

[26] W. Bahsoun, Nonlinearity, **19**, 2529, (2006).

[27] W. Bahsoun, C. Bose and Y. Duan, arXiv:1301.4033 [math.DS], (2013).

[28] G. Froyland, Nonlinearity, **12**, 79, (1999).

[29] G. Froyland, Nonlinearity, **12**, 1029, (1999).

[30] W. Bahsoun and C. Bose, Nonlinear Anal.: Theo., Meth. and Appl., **74**, 4481, (2011).

[31] M. F. Demers, P. Wright and L-S Young, Commun. Math. Phys. **294**, 353, (2010).

[32] A. Nemeth and P. Szepfalusy, Phys. Rev. E, **52**, 1544, (1995).

[33] H. Lustfeld and P. Szepfalusy, Phys. Rev. E, **53**, 5882, (1996).